40

Monte Carlo Simulations of Adsorbed Molecules on Ionic Surfaces

Abdulwahab Khalil Sallabi
Misurata University
Libya

1. Introduction

Monte Carlo (MC) method [1-10] refers to all calculations that involve the use of random numbers for sampling processes of approximate solutions to quantitative problems. It can be applied for application domains range from economics to physics to chemistry to surface science to medicine.
The Monte Carlo (MC) method is usually Linked to Comte de Buffon a French eighteenth-century naturalist, who performed an experiment by throwing a needle of length ℓ at random onto a board marked with parallel lines a distance d apart to infer the probability p that the needle will intersect one of those lines. Búffon's subsequent experiments enabled him to make an accurate estimation of π. Following the procedure of Buffon, Laplace, and then In 1864, Captain O. C. Fox and in 1873, A. Hall [8] used Monte Carlo method calculate π.
Early 1940's marked the beginning of the modern history of Monte Carlo when scientists at Los Alamos systematically used them as a research tool in their work on developing nuclear weapons. Stanislaw Ulam was the first one to realize the potential of using computers to automate the statistical sampling process. Stanislaw Ulam, John von Neuman and Nicolas Metropolis developed algorithms and explored the means to convert non-random problems into random forms so that statistical sampling can be used for their solution. The name "Monte Carlo" was suggested by Metropolis after the famous Monaco casino. One of the first published papers on this topic was by Metropolis and Ulam in 1949 [9].

2. Metropolis Monte Carlo method

Nicolas Metropolis introduced the Metropolis Monte Carlo method at the dawn of the computer era in 1953 [10]. The rapid development in computer technology has increased the applicability and accuracy of the Monte Carlo method and is now used routinely in many diverse fields, such as economics, physics and chemistry as a powerful numerical technique. As we know, it is easy to solve equations of interaction between two atoms or molecules and get an exact solution for a specific problem while in the case of large systems, where the number of particles involved in a problem is large, solving the problem in a deterministic way becomes impossible due to the large number of equations and variables that are needed to study the problem. Monte Carlo (MC) methods are stochastic (random) techniques in which random numbers and probability statistics are used to examine scientific problems in a probabilistic fashion rather than a deterministic one. To study the physical properties of a

system with a large number of atoms or molecules interacting with each other, MC methods can be readily applied whereby possible configurations of the system can be sampled according to their Boltzmann probability distribution via the use of random numbers [1] [3] [11] [12].

Metropolis Monte Carlo simulations have been performed to study the structures and phase transitions of adsorbed molecules on solid surfaces such as HBr/LiF(001) [13], CO_2/NaCl [14], CO/NaCl [15], CO/LiF [16], CO/MgO [17], N_2/NaCl [18], N_2/LiF [19], H_2/NaCl [20], D_2/MgO [21], H_2/LiF [22,23]. They have also been used to study critical phenomena near their transition temperatures for many models such as the Ising, XY, and Heisenberg models [12]. MC methods have proved to be useful tools since they allow for the sampling of a large number of possible configurations at nonzero temperatures.

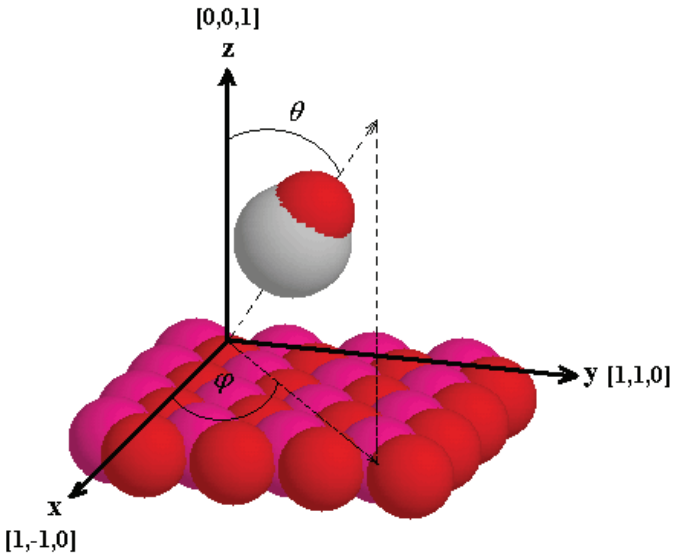

Fig. 1. A view of the angular coordinate system with respect to the xyz coordinate system. The polar angle θ is the tilt of the molecular axis (carbon to oxygen) with respect to the surface normal (z-axis) while the azimuthal angle φ is the angle between the x-axis and the projection of the molecular axis onto the plane of the surface (xy-plane).

By using the Metropolis Monte Carlo (canonical ensemble or Q(N,V,T)) technique [10], we can simulate the interaction of adsorbed molecules on ionic surfaces, where the number of molecules N, the simulation volume V, and temperature T are fixed during any simulation. In other words, during a simulation the positions and the orientations of molecules are allowed to change while the number of molecules, volume and temperature are not allowed to change. A MC simulation is typically broken down into cycles. In every cycle, each adsorbed molecule is allowed to move in a random fashion. In each move a randomly chosen molecule is moved to a new random position or orientation. Then the computer decides whether to accept or reject this move with a Boltzmann probability $\exp(-\Delta E / k_B T)$ that depends on the change in energy ($\Delta E = E_{new} - E_{old}$) of the new ($E_{new}$) and old ($E_{old}$) configuration. This process is repeated many times until there is no further change in the

average energy and other computed properties of the system, at which point the system is deemed to have reached thermodynamic equilibrium. After this point is reached, a large number of configurations (geometries) are accumulated and the data are averaged to obtain thermodynamic properties of the system, such as the energy and angular distributions. An example of one of the coordinate systems which can be used to describe the adsorbed molecules is shown in Fig. 1, in this coordinate system the position of an adsorbed molecule is described by the position vector **r**(x,y,z) with respect to the origin which is taken in the plane z=0 (the surface of the substrate) and at the anion site with the x and y axes running along the [1,-1,0] and [1,1,0] crystallographic directions respectively and with the z axis set perpendicular to the surface. The orientation of an adsorbed molecule is described by a polar angle θ and an azimuthal angle φ. In Fig. 2 we show the general steps of the Metropolis Monte Carlo simulation [24].

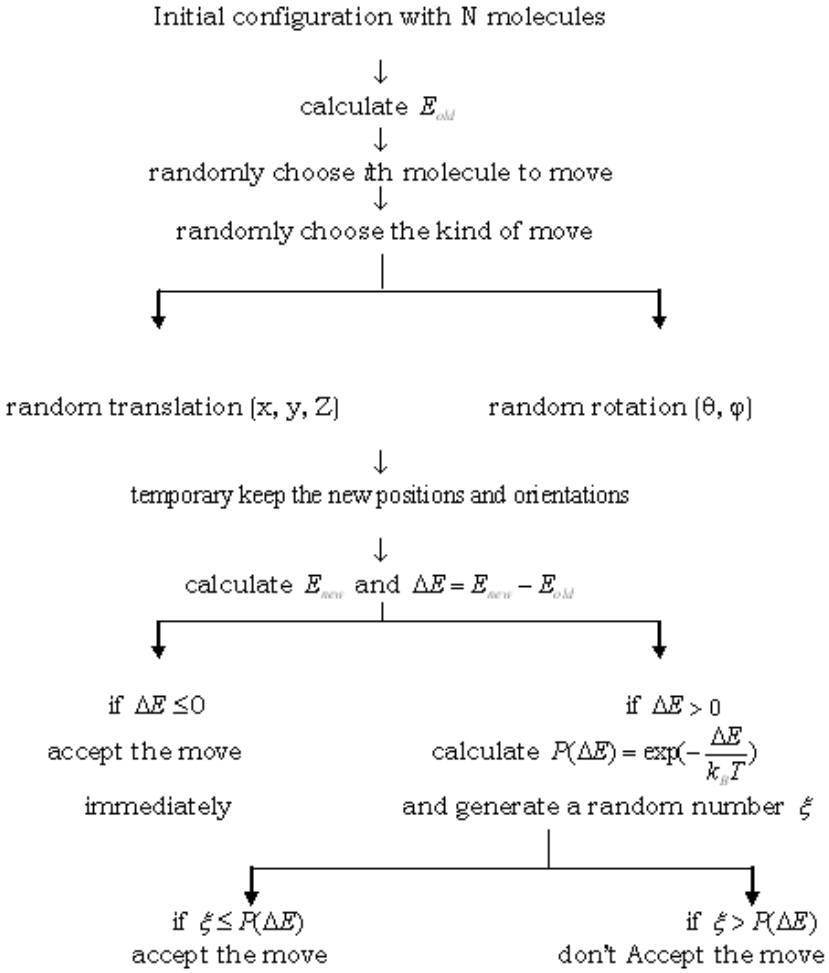

Fig. 2. Flow chart of general steps of Metropolis Monte Carlo method

During the simulations an ensemble of N adsorbed molecules are placed in the surface potential of the ionic substrate. The surface potential is fixed in the space. If all of the positive sites of the surface are occupied then a monolayer of adsorbed molecules is formed. Periodic boundary conditions in the lateral directions (x and y) were imposed as well as a cutoff radius for the molecule-molecule interactions. Each move is subjected to the usual Boltzmann weighted acceptance criterion. The amplitudes of the moves were adjusted independently and maintained a 50% acceptance probability. Statistics were collected after the system is equilibrated. In the case of studying critical phenomena, analysis near the critical temperature needs very long runs to obtain good results.

3. Statistics

In order to study the continuous phase transition expected for the some of the adsorbed molecules on ionic surface (e.g.. N_2 on NaCl..) we need to calculate statistically the average energy (E), heat capacity (C_v), order parameter (Φ) and susceptibility (χ) for a monolayer of adsorbed molecules on a square lattice with LxL=N sites. To do that the order parameter and the energy per molecule were collected every cycle and have been kept for further analysis. The heat capacity per particle is obtained from the fluctuations in the monolayer energy E *via* [24],

$$C_v=(\langle E^2\rangle-\langle E\rangle^2)/Nk_BT^2 \tag{1}$$

The order parameter Φ tells us how well the system is ordered. When the system is perfectly ordered the order parameter has a value of one while it has a value of zero when the system is fully disordered. The order parameter Φ for an anti-ferromagnetic like ground state is defined in terms of the azimuthal angle φ through the following relations and transformations [25].

$$\Phi = \sqrt{\Phi_x^2 + \Phi_y^2} \tag{2}$$

$$\Phi_x = N^{-1} \sum_{i=1}^{N} (-1)^{n_{yi}} \cos(\varphi_i) \tag{3}$$

$$\Phi_y = N^{-1} \sum_{i=1}^{N} (-1)^{n_{xi}} \cos(\varphi_i) \tag{4}$$

where n_{xi}=1,2,3,…,L and n_{yi}=1,2,3,…L, label the x and y positions of the adsorption sites of molecule *i* on the lattice. The summations are taken over all the localized adsorption sites of the molecules on a square lattice from 1 to $N=L^2$. The transformed order parameter [146] Φ is obtained by using the phase factors $(-1)^{n}xi$ and $(-1)^{n}yi$. If the configuration of the adsorbed molecules is of the antiferro-type then the transformed configuration will be ferro-type where all the adsorbed molecules are oriented in the same direction. It is worth noting that these transformations don't affect the orientation of the adsorbed molecules in the Monte Carlo program. The process of transformation is temporarily made after every Monte Carlo move when the order parameter is calculated. The susceptibility is constructed from fluctuations in the order parameter, *via*.

$$\chi = \left[\left\langle \Phi^2 \right\rangle - \left\langle \Phi \right\rangle^2 \right] N / k_B T \tag{5}$$

To determine how often we should sample a set of available data (X), in order to calculate quantities such as the average energy, heat capacity and order parameter, an examination of the autocorrelation function [142] of data {X) can be used,

$$C(\tau) = \frac{\left\langle X_i X_{i+\tau} \right\rangle - \left\langle X_i \right\rangle^2}{\left\langle X_i^2 \right\rangle - \left\langle X_i \right\rangle^2} \tag{6}$$

where X_i is the value of X at cycle i. The autocorrelation function for a number τ of steps can be calculated. It has a value of one when the data are completely correlated ($\tau = 0$) and decays exponentially to zero as τ becomes large enough that the data became uncorrelated. We can then find the number of steps (τ_e) required for the autocorrelation function C(τ) to decay to 0.367 (1/e) of its value at $\tau = 0$. The data X can then be sampled every (τ_e) steps and still be uncorrelated. Phase transitions in real systems (in experiments) are considered to be in the thermodynamic limit and thus effectively infinite in size. In computer simulations, the sizes of adsorbed systems are finite and small compared to the sizes of the real systems. It has been proved that, in the finite systems used in computer simulations the phase transition temperature is shifted compared to the phase transition in the real systems. Hence, the transition temperature $T_c(L)$ changes as the 2-d size $L \times L$ of the system changes. This, plus the presence of large fluctuations due to finite size effects, makes it difficult to determine $T_c(\infty)$. In order to overcome these problems in determining the transition temperature for a system of infinite size, the Binder fourth order cumulant [26] [27]

$$U_L(T) = 1 - \frac{\left\langle \Phi^4 \right\rangle_L}{3\left\langle \Phi^2 \right\rangle_L^2} \tag{7}$$

for several values of L can be used to locate the transition point for a system of infinite size. When U_L is plotted as a function of temperature for a several systems of different sizes, we will get a set of curves that intersect at the infinite size transition temperature where they are independent of the lattice size. The fourth order cumulant has two limiting values, for a completely ordered system U_L=2/3, while U_L=0 when the system is completely disordered. As the system size is increased, the fourth order cumulant will have values close to these limits.

4. Interaction potentials

To simulate the systems of interest of molecules on ionic surfaces, the potential energy functions must be constructed to calculate the total potential energy of the system to be simulated. The total potential consists of two parts, molecule-molecule and molecule-surface potentials. Our ability to reproduce known experiments data depends greatly on the parameters used to calculate the potential energy. Usually atom-atom/ion potentials with summation over a two body interactions is applied to describe the repulsion and dispersion interactions. In addition to these interactions, electrostatic contributions are also considered in similar way [1][29][28].

4.1 Molecule-molecule interactions

Site-site model could be used to construct the intermolecular potential. The parameters governing the potentials are chosen so as to reproduce various experimental molecular

4.1.1 Electrostatic interactions

The electrostatic interactions are mediated by point charges q_i and point dipoles $\vec{\mu}$ i that are distributed around the molecule (on the atomic sites) in such a way that the known multipole moments of the molecule can be reproduced through the following linear equations [92],

$$q_1 + q_2 = 0 \tag{8}$$

$$\mu = \sum_{i=1}^{2} q_i r_i + \sum_{i=1}^{2} \mu_i \tag{9}$$

$$\Theta = \sum_{i=1}^{2} q_i r_i^2 + 2\sum_{i=1}^{2} \mu_i r_i \tag{10}$$

$$\Omega = \sum_{i=1}^{2} q_i r_i^3 + 3\sum_{i=1}^{2} \mu_i r_i^2 \tag{11}$$

$$\Lambda = \sum_{i=1}^{2} q_i r_i^4 + 4\sum_{i=1}^{2} \mu_i r_i^3 \tag{12}$$

where μ Θ Ω and Λ are the molecular dipole, quadrupole, octupole and hexadecapole moments respectively. The r_i are the distances of the point charges q_i and point dipoles μ_i at site i from the molecular center of mass. The values of the distributed point charges and dipoles at the atomic sites can be determined by using the above equations. The electrostatic interactions between an atom i (with charge q_i and dipole μ_i) of a molecule "m" with an atom j of another molecule "n" (with charge q_j and dipole μ_j) can be written as follows [96],

$$V_{ij}^{(elc)} = \frac{q_i q_j}{r_{ij}} - \frac{q_i \mu_j}{r_{ij}^3}\left(\hat{u}_j \cdot \vec{r}_{ij}\right) + \frac{q_j \mu_i}{r_{ij}^3}\left(\hat{u}_i \cdot \vec{r}_{ij}\right) + \frac{\mu_j \mu_i}{r_{ij}^5}\left[\left(\hat{u}_i \cdot \hat{u}_j\right) r_{ij}^2 - 3\left(\hat{u}_i \cdot \vec{r}_{ij}\right)\left(\hat{u}_j \cdot \vec{r}_{ij}\right)\right] \tag{13}$$

where $\vec{r}_{ij}$ is the vector position of i^{th} atom of the n^{th} molecule with respect to the j^{th} atom of the m^{th} molecule. In other words, $\vec{r}_{ij}$ points from atom j to atom i. And $\hat{u}_i$ is an orientation unit vector of n^{th} molecule.

4.1.2 Van der Waals interactions

Once again the atomic site model is usually used to model the van der Waals interaction (repulsion and dispersion interaction) between molecules so that, the molecular interaction may be expressed in terms of the atom-atom interactions by the modified Buckingham potential.

$$V_{ij}(r_{ij}) = A_{ij}\exp(-\eta_{ij}r_{ij}) - \frac{C_6^{ij}}{r_{ij}^6} - \frac{C_8^{ij}}{r_{ij}^8} \tag{14}$$

where the variable r_{ij} is the distance between atom sites *i* and *j* of different molecules. The Born-Mayer parameters, A_{ij} and η_{ij}, characterize the strength and the range of the repulsion respectively. C_6 and C_8 are dispersion constants that represent the strength of the leading terms in the dispersion series, these constants are well known for molecules and are easy to determine for atomic sites. In contrast, the repulsive parameters are difficult to obtain experimentally in most cases and hence the repulsive parameters can be adjusted so as to reproduce certain experimentally known quantities such as the crystal structure and cohesive energy of molecules on ionic surface. Known radii (a_i) and softness (b_i) parameters are used to construct the Born-Mayer parameters as follows [30],

$$\eta_{ij} = \frac{1}{b_i + b_j} \tag{15}$$

$$A_{ij} = \left(b_i + b_j\right) exp\left(\frac{a_i + a_j}{b_i + b_j}\right) \tag{16}$$

In order to use the site-site model, the molecular dispersion interaction parameters, available in the literature for the molecules must be broken up into atomic based ones [31] [32],

4.2 Molecule-surface interaction

The pairwise sum of two-body interactions (atom-ion interactions) could be used to model the electrostatic, dispersion and repulsion interactions between a molecule and the substrate. Because we are dealing with physisorbed systems where there is no noticeable reconstruction or distortion of the (001) ionic surface [33], it reasonable to assume that the surface of the substrate is not perturbed by adsorbed molecules and hence has the same lattice constant as the bulk. Ions of the surface are considered to be periodic in two dimensions and regular (the substrate is regarded as a semi-infinite solid) in the third dimension

4.2.1 Electrostatic interactions

The electrostatic energy (V_{elc}^{m-s}) of a single diatomic molecule on the ionic surface can have the following form

$$V_{elc}^{m-s} = \sum_{i=1}^{2}\left(\psi\left(\vec{r}_i\right)q_i + \vec{E}\left(\vec{r}_i\right)\cdot\vec{\mu}_i - \frac{1}{2}\alpha_i^{\perp}E_{\perp}^2\left(\vec{r}_i\right) - \frac{1}{2}\alpha_i^{\parallel}E_{\parallel}^2\left(\vec{r}_i\right)\right) \tag{17}$$

Where q_i, $\vec{\mu}_i$ are point charges and point dipoles at the atomic sites of the molecule. $\psi(\vec{r}_i)$ and $\vec{E}(\vec{r}_i)$ are the electrostatic potential and electric field generated by the ionic crystal at position $\vec{r}$, the location of the interacting atom with respect to the origin of the coordinate system. The induction energy, which depends upon the "atomic" polarizabilities

(perpendicular ($\alpha_i^{\perp}$) and parallel ($\alpha_i^{\parallel}$) to the molecular axis), is included in our calculations.

The sum in the above equation is over the two atomic sites of the diatomic molecule. The electrostatic potential above the surface of a FCC ionic crystal is well known [34] and may be written as a two dimensional Fourier series whose leading term is [35]

$$\psi(\vec{r}_i) = -\frac{4e}{a}\left[\frac{\exp\left(-\frac{2\pi z}{a}\right)}{1+\exp\left(-\sqrt{2}\pi\right)}\right]\left(\cos\left(\frac{2\pi x}{a}\right)+\cos\left(\frac{2\pi y}{a}\right)\right) \tag{18}$$

where *e* is the absolute value of the electronic charge on an individual ion and *a* is the lattice constant of the surface mesh. The electric field at the crystal surface is readily calculated from the gradient of the electrostatic potential,

$$\vec{E}(\vec{r}) = -\vec{\nabla}\psi(\vec{r}) \tag{19}$$

4.2.2 Van der Waals interactions

The Tang-Toennies potential is used to describe the repulsion and dispersion interaction of an atom of an adsorbed molecule with an ion of the substrate,

$$V_{ij}^{m-s}(r_{ij}) = A_{ij}\exp(-\eta_{ij}r_{ij}) - \sum_{n=3}^{\infty} f_{2n}(r_{ij})\frac{C_{2n}^{ij}}{r_{ij}^{2n}} \tag{20}$$

where r_{ij} is the distance of atom *i* to ion *j* and C_6, C_8 and C_{10} are the atom-ion dispersion coefficients. The mathematical singularities at r=0 are removed by the presence of the phenomenological damping functions

$$f_{2n}(r_{ij}) = 1 - \sum_{k=0}^{2n}\frac{\left(\eta_{ij}r_{ij}\right)^k}{k!}\exp(-\eta_{ij}r_{ij}) \tag{21}$$

The dispersion series is in principal infinite but some times for practical reasons is truncated at the k=5 term, *i.e.* only the C_6, C_8 and C_{10} terms are included. To fully describe the potential it was necessary to estimate all interaction parameters A_{ij}, η_{ij}, C_6, C_8 and C_{10} for each of the atom-ion interactions.

4.2.2.1 Dispersion parameters

Values of C_6, C_8 and C_{10} for the molecule-ion interactions can be estimated from combining rules derived [36] [37]. For example, the C_6 are assumed to obey the following relation

$$C_6^{ij} = \frac{2C_6^{ii}C_6^{jj}\alpha^i\alpha^j}{C_6^{ii}\left(\alpha^j\right)^2 + C_6^{jj}\left(\alpha^i\right)^2} \tag{22}$$

where the index *i* refers to the molecule and *j* refers to either the positive or negative ion in the substrate, and α is average polarizability. The values of C_8 can be found using the following relations [36]:

$$C_8^{ij} = C^{ij}(1,2) + C^{ij}(2,1) \tag{23}$$

Where,

$$C^{ij}(1,2) = \frac{15}{4}\left[\frac{\alpha_1^i \alpha_2^j Y_1^i Y_2^j}{Y_1^i + Y_2^j}\right] \tag{24}$$

$$Y_1^i = \frac{4}{3}\frac{C_6^i}{\left(\alpha_1^i\right)^2} \tag{25}$$

$$Y_2^i = \frac{2C_8^i Y_1^i}{15\alpha_1^i \alpha_2^i - 2C_8^i} \tag{26}$$

$$C_6^{ij} = \frac{2C_6^{ii} C_6^{jj} \alpha^i \alpha^j}{C_6^{ii}\left(\alpha^j\right)^2 + C_6^{jj}\left(\alpha^i\right)^2} \tag{27}$$

The values of the C_{10} coefficients for each of the molecule-ion pairs were estimated using the approximate relation [38]

$$C_{10} = 49(C_8)^2 / 40C_6 \tag{28}$$

These values of the molecule-ion dispersion coefficients C_6, C_8, and C_{10} were used to calculate the atom-ion dispersion coefficients

$$C_6^{\text{atom-ion}} = \left(\alpha_{\text{atom}} \Big/ \alpha_{\text{molecule}}\right) C_6^{\text{molecule-ion}} \tag{29}$$

4.2.2.1 Repulsion parameters

The method used to obtain Born-Mayer parameters for the atom-ion interactions are identical to that used in Ref. 29. The Born-Mayer parameters for atom-ion interactions are estimated by using the combining rules of Gilbert [39] [40] and Smith [41]

$$A_{ij} = \left[\frac{\eta_{ii} + \eta_{jj}}{2\eta_{ii}\eta_{jj}}\right]\left(A_{ii}\eta_{ii}\right)^c \left(A_{jj}\eta_{jj}\right)^d \tag{30}$$

Where,

$$\eta_{ij} = \frac{2\eta_{ii}\eta_{jj}}{\left(\eta_{ii} + \eta_{jj}\right)} \tag{31}$$

$$c = \frac{\eta_{jj}}{\eta_{ii} + \eta_{jj}} \tag{32}$$

$$d = \frac{\eta_{ii}}{\eta_{ii} + \eta_{jj}} \tag{33}$$

5. Monte Carlo results

A great deal of understanding of the fundamental processes in surface science comes through the use various experimental and computational studies of adsorbed layers on various solid surfaces, e.g. the theory of interactions of gases with solid surfaces [1][2], orientational ordering of adsorbed layers, e.g. diatomic molecules on graphite [3][4][5], thin films on solid surfaces [6], surface diffusion [7], surface aligned photochemistry [8][9], phase transitions and critical phenomena, e.g. 4He on graphite [10][11], 4He on Kr-preplated graphite [12], and the structures and dynamics of molecules on ionic surfaces [13].
Parallel to the experimental techniques such as low energy electron diffraction (LEED)[14], helium atom scattering (HAS)[15][16], polarization infrared spectroscopy (PIRS)[17] and Calorimetric, computer simulations have been accepted as a useful tool in determining additional details of the structures of adsorbed molecules. Thus they help in understanding physics at surfaces [20][21], and have been used to substantiate and interpret experimental results [22-26]. Furthermore, computer simulations can be used to predict additional results and guide experiments to perform more experimental work [5][27]. The most widely known techniques in computer simulation are the Metropolis Monte Carlo (MC) [26-29] and Molecular Dynamics (MD) methods [21].

5.1 N_2 and CO on NaCl(001) and LiF(001)

Monte Carlo simulations have been used to study the structures and phase transitions of CO/NaCl(001), CO/LiF(001) and N_2/NaCl(001) systems [15][16][18]. Through the use of Monte Carlo simulations, these systems have been identified as falling into the class of phase transition whose critical exponents are nonuniversal.
What makes the critical exponents interesting is the idea of universality. The critical exponents are found to be independent of the details of the interatomic interactions. According to the idea of universality, the critical exponents of all systems that exhibit a continuous phase transition near the critical temperature can be grouped into a small number of universality classes. Within each universality class, the critical behavior is remarkably similar. In Table 1 the universality classes, which are related to the order-disorder phase transitions in two dimensions are presented.
In two dimensional systems there is a symmetry class whose critical exponents have nonuniversal values [43-46]. The values of the exponents in this class depend on the strengths of an anisotropic external potential h4. In CO/NaCl(001), CO/LiF(001) and N_2/NaCl(001) systems this anisotropy is provided by the substrate and perhaps the molecule-molecule interactions. As shown in Fig.3, for infinite anisotropy the Ising exponents are recovered whereas in the limit of zero anisotropy Kosterlitz-Thouless (K-T) behaviour occurs. For example, the critical exponent β, has a value of 0.125 for the Ising model (infinite anisotropy) and will increase towards infinity as K-T behaviour is

approached at zero anisotropy. The critical exponents α, β, and γ are associated, respectively, with the critical behaviour of the heat capacity C_v, order parameter Φ, and susceptibility χ as follows: $C_v \sim A^{\pm} \cdot t^{-\alpha}$, $\Phi \sim B^{-} \cdot t^{\beta}$, and $\chi \sim C^{\pm} \cdot t^{-\gamma}$, where the reduced temperature is defined as $t = |(T_c - T)/T_c|$ and the amplitudes $A^{\pm}$, $B^{\pm}$, and $C^{\pm}$ carry a positive (negative) superscript for the temperatures above (below) T_c. With values of α, β and γ in hand it is possible to check the validity of Rushbrooke's relation, $\alpha + 2\beta + \gamma \geq 2$.

Universality class Exponent	Ising	XY with cubic anisotropy	3-state Potts	4-state Potts
α	O (log)	Non universal	1/3	2/3
β	1/8	Non universal	1/9	1/12
γ	7/4	Non universal	13/9	7/6

Table 1.1 Universality classes and its critical exponents.

Monte Carlo (MC) simulations have provided details of the ordered monolayer structure and successfully reproduced the transition to the disordered state at temperatures around 30–35 K in the CO/NaCl(001) system [15]. It was argued that these phase transitions are of interest because they fall into the universality class of the XY model with cubic anisotropy and hence should have nonuniversal critical exponents, i.e., their values depend on the relative strengths of an anisotropic external potential provided by the substrate and the molecule molecule interactions.

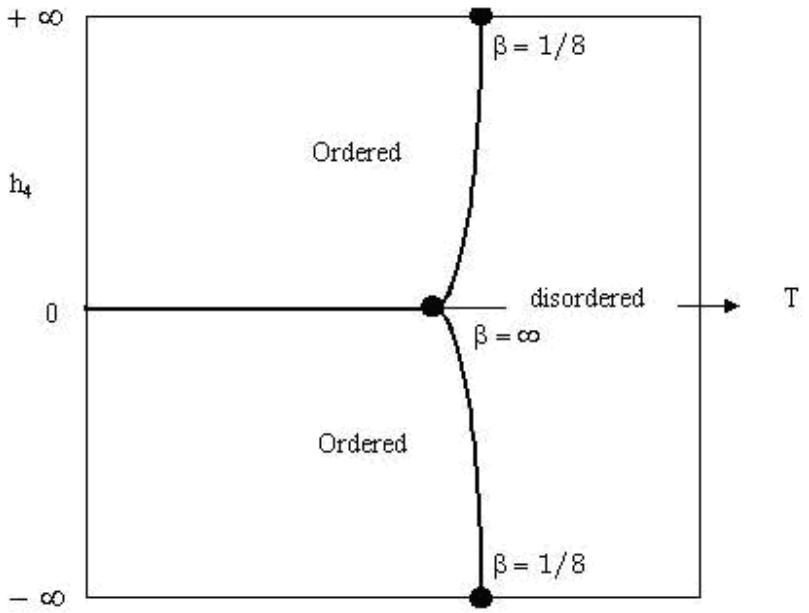

Fig. 3. Phase diagram for the XY model in the h4 –T plane shows how the critical exponent β varies with anisotropy strength h4 (Ref. [43]).

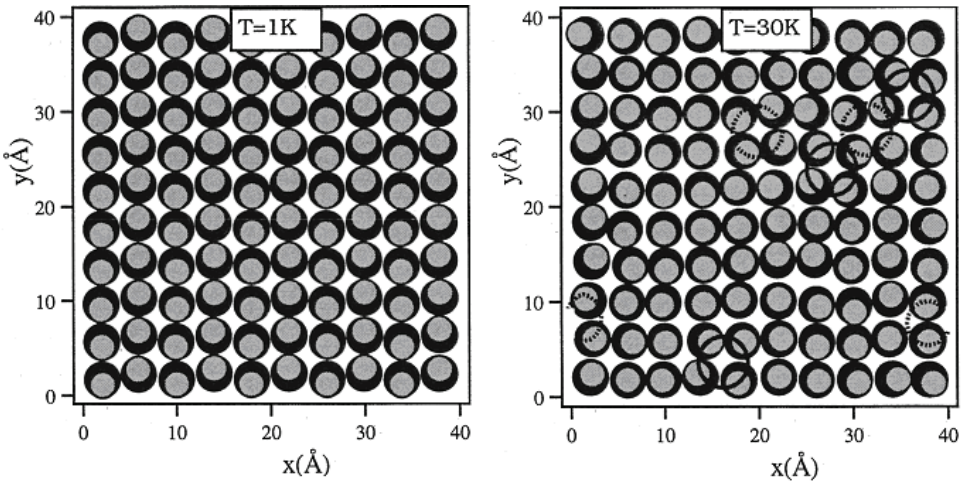

Fig. 4. An overview of a typical configuration of 100 N_2 molecules at 1 K and 30 K. The nitrogen atoms closest to the surface are shown as black and the upper nitrogen atoms as gray. Clockwise (counterclockwise) vortices are denoted by the solid (dashed) circles. (this figure taken from Ref [18])

Metropolis Monte Carlo (canonical ensemble) simulations of the N_2 /NaCl(001) [18] system is predict that at low temperatures a monolayer of nitrogen molecules forms an ordered p(2×1) structure which, upon heating past 25 K, undergoes an order-disorder phase transition as shown in Fig. 4. In the disordered phase the long-range orientational order among molecules is destroyed although residual shortrange order persists in the form of small ordered domains and pairs of counter rotating vortices. The destruction of orientational order is further shown in Fig. 5, where the azimuthal angle distributions are plotted for several temperatures. The distributions are sharply peaked at $\pm 90°$ at low temperatures and broaden as the temperature increases. Around 25 K the distribution becomes uniform indicating a loss of long-range azimuthal order and signaling a transition to a disordered phase. However, minor residual peaks at $\varphi = \pm 90$, are still observed at T=30 K. As one might expect, this overall behavior is similar to that of the CO/NaCl system with differences occurring in the details, such as the values of the transition temperature and tilt angle. The heat capacity of the N_2 /NaCl(001) was found to have a maximum at 25.0 K and exhibit a logarithmic type divergence that can be expressed as

$$C-/R=-0.256\ \ln(t)-0.158+2.5 \text{ for } T<Tc, \tag{34}$$

$$C+/R=-0.250\ \ln(t)-0.200+2.5 \text{ for } T>Tc, \tag{35}$$

where the background heat capacity of 2.5R, due to the presence of three translational and two rotational modes, is shown explicitly. The slopes are close to those reported previously. The heat capacity data was also analyzed as a power law divergence and a value of α=0.076±0.010 was found [18].

The adsorption of N_2 on the LiF(0 0 1) surface is studied by canonical Monte Carlo (CMC) computer simulation [19]. As shown in Fig. 6, these studies predicted that N_2 forms an ordered structure where the molecules are arranged in a unit cell of $p(2\sqrt{2}\times\sqrt{2})R45^\circ$

symmetry at temperatures below 23 K with 50% coverage. As shown in Fig. 7, the nitrogen molecules are tilted by 53° from the surface normal and have the same azimuthal orientation along diagonals, with diagonals alternating their orientation see Fig. 7. Beyond 23 K, the molecules become azimuthally disordered but with residual short-range order. No change in the position of the peak of the polar (tilt) angle distribution was observed above the transition temperature. This transition is purely of the order–disorder type.

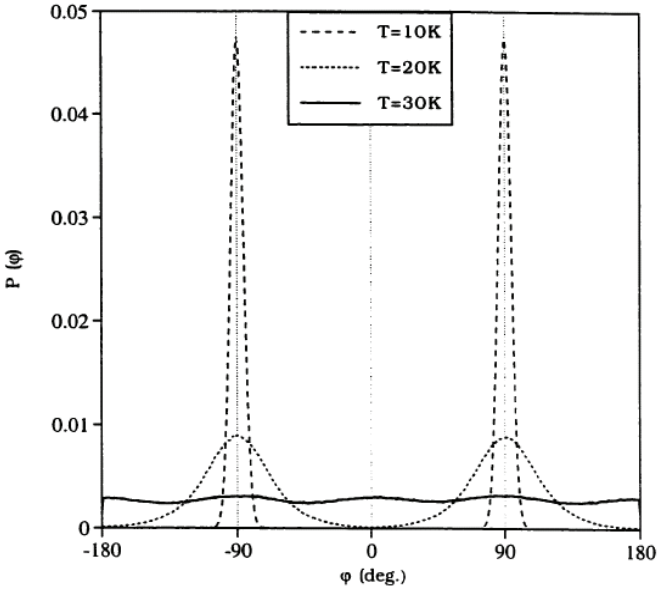

Fig. 5. The azimuthal angle (φ) distribution is plotted for temperatures T=10, 20, 30 K. At 1K the distributions are symmetric and centered on the θ ~0°, 31°. As the temperature increases this peak decreases in height and broadens in width. The peak centered on θ ~31° at 1K shifts below to θ ~28° at 40 K.

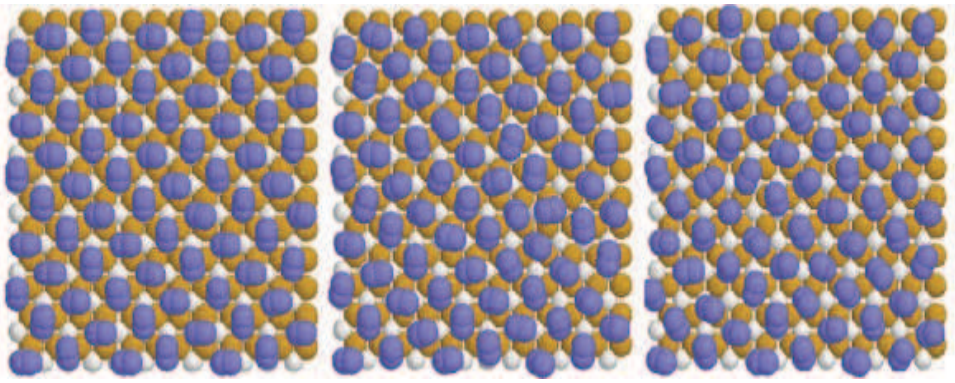

Fig. 6. The final configurations of a monolayer of N_2 on LiF(001) surface at 1 K (left), 20 K (middle) and 25 K (right). The monolayer at 1K forms an ordered $p(2\sqrt{2}\times\sqrt{2})R45^{\circ}$ structure

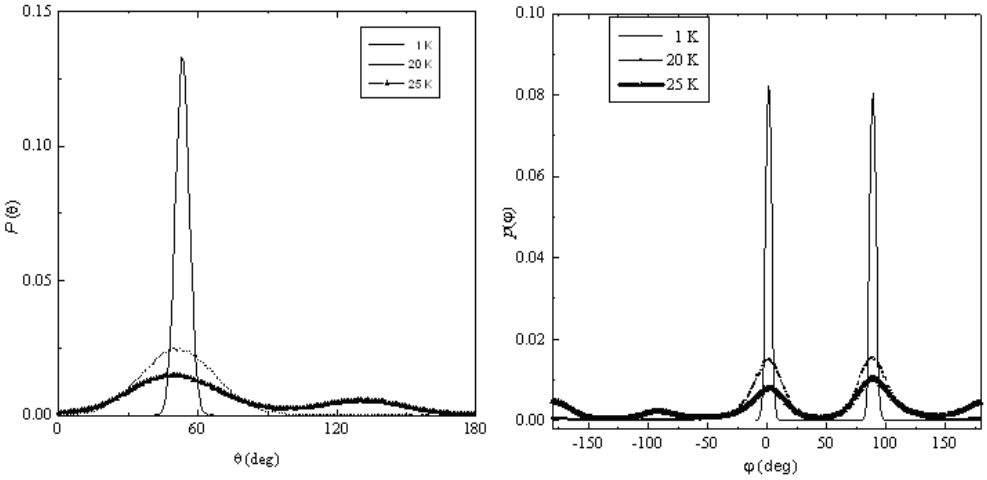

Fig. 7. Polar angle (left) distribution is plotted for temperature T = 1 K, 20 K and 25 K. At 1 K the distribution is symmetric and centered at 53°. Azimuthal angle (φ) distributions (right) of the N_2 molecules adsorbed on LiF surface at 1 K, 20 K and 25 K show the progress of the transition from an ordered to a disordered phase.

5.2 CO on MgO(001)

Monte Carlo simulations of CO [17] show that below 41 K the CO molecules form a c(4×2) structure with six molecules per unit cell distributed into two kinds of adsorption sites as shown in Fig. 8: a perpendicular site and a tilted site (polar angle of 31°). Both sites are localized near Mg^{2+} ions. The occupancy of perpendicular sites to tilted sites occurs in the ratio of 1:2. At 41 K the *c*(4×2) phase undergoes a phase transition into a less dense, disordered phase accompanied by the expulsion of some molecules to form a partial second layer. The density of the remaining disordered layer is the same as for a *p*(3×2) phase and portions of the disordered layer show regions of short range ordering with either the c(4×2) or *p*(3×2) structures. The *p*(3×2) phase contains four molecules per unit cell and also consists of perpendicular and tilted sites, but in the ratio of 1:1. This structure was found to be stable up to 50 K after which the expulsion of some molecules and disordering of the layer occurred. A model to test the relative stability of these two phases by examining the difference in Gibbs free energy is constructed and shows that below 41 K the *c*(4×2) phase is the most stable but above 41 K the *p*(3×2) phase is the most stable. However, at low pressures the model suggests that the *p*(3×2) phase will not be observed and the layer will instead transform from the c(4×2) phase to a disordered phase at 41 K. This result reconciles the findings of low-energy electron diffraction (LEED) experiments *p*(3×2) phase observed] with those of helium atom scattering (HAS) and polarization infrared spectroscopy (PIRS) experiments (disordered phase observed). It is proposed that the c(4×2)-->p(3×2) transition is part of an infinite sequence of transitions involving (n×2)-type structures which, under suitable conditions of temperature and pressure, constitutes an example of the devil's staircase phenomenon. Such a phenomenon has been suggested by previous LEED experiments.

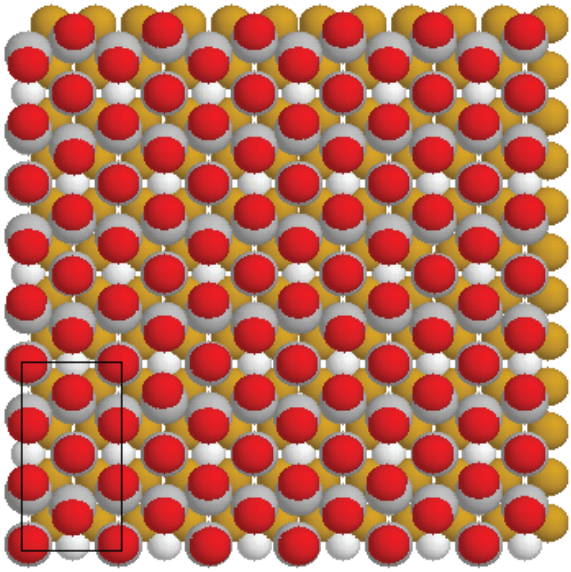

Fig. 8. A top view of the MgO(100) surface covered with 108 CO molecules at 1 K. The carbon atoms are shown as white and the oxygen atoms as red. The small white ball represents a Mg ion and orange ball represents a O ion. Note that the origin is centered on a O ion. The resulting $c(4\times2)$ unit cell is shown (solid lines).

5.3 H_2 and D_2 on NaCl(001), LiF(001) and MgO(001)

A Monte Carlo simulation is used to study the H_2 and D_2 molecules adsorbed on a NaCl(001), LiF(001) and MgO(001) surfaces [20-23]. In the case of H_2 on NaCl(001), (Fig. 10) H_2 forms a commensurate c(2×2) structure where the hydrogen molecules sit flat on top of the cationic Na+ sites. The unit cell was found to have four molecules, where pairs of neighboring molecules are aligned perpendicular to each other in a "T" configuration. This structure is in agreement with the experimental results in terms of coverage and stability, but disagrees in terms of symmetry since the PIRS-ATR and HAS experimental results show a (1×1) structure. To solve this problem, the rotational motion of H_2 molecules has been studied using perturbation theory and it is found that quantum effects will azimuthally delocalize the orientation of the molecular axis of H_2. Thus, the c(2×2) structure becomes a (1×1) structure. These simulations also show that a second layer is possible, where all hydrogen molecules adsorb over the anionic sites in a unit cell of $p(2\times1)$ symmetry. Perturbation Theory calculations show that p-H2 and o-H_2 (J=1, m=±1) prefer to sit on the top of Na+ site, while o-H_2 (J=1, m=0) prefers to locate over the Cl^- site. Monte Carlo (MC) simulations of D_2 molecules on the MgO(001) surface are reported and show that a series of interesting structures form with increasing coverage, viz. $p(2\times2) \rightarrow p(4\times2) \rightarrow p(6\times2)$, with coverages Θ = 0.5, 0.75, and 0.83 respectively, and are stable up to 13 K. The $p(2\times2)$ structures contain two D_2 molecules per unit cell, with each molecule lying parallel to the plane of the surface (θ = 90°) directly above every other Mg^{2+} site. The molecules adopt a "T" configuration with respect to their nearest neighbors. The $p(4\times2)$ and $p(6\times2)$ structures,

have two kinds of adsorption sites: a parallel site, as in the case of $p(2\times2)$, and a tilted site, where the D_2 molecules sit between cationic and anionic sites with the molecular axis directed towards the anionic site, with $\theta \approx 60°$. These structures are consistent with recent Neutron Scattering results in terms of coverage and stability, but disagree in terms of symmetry; the neutron scattering work found "c" type structures whereas the MC simulations (without quantum considerations) yield a "*p*" type structures. To reconcile the results of the simulations and experiments, the quantum mechanical rotational motion of the adsorbed D2 molecules was studied using perturbation theory. These calculations show that the adsorbed D_2 molecules are azimuthally delocalized and hence the structures are indeed "c" type rather than "p" type.

Monte Carlo (MC) simulations has been preformed for H_2 on LiF(001). MC simulations predict that H_2 molecules form a series of interesting structures, $p(2\times2) \rightarrow p(8\times2) \rightarrow p(4\times2)$ with coverages Θ=0.5, 0.625 and 0.75 respectively, that are stable up to 8 K (see Fig. 11). These structures are consistent with recent Helium Atom Scattering results (the $p(4\times2)$ is not observed) in terms of coverage and stability, but disagree in terms of symmetry. The HAS work found "c" type structures whereas the Metropolis MC simulations yield a "p" type structures. To reconcile the results of the simulations and experiments, the rotational motion of the adsorbed H_2 molecules was studied using perturbation theory. These calculations show that the adsorbed H2 molecules are azimuthally delocalized and hence the structures are indeed c-type. Our calculations also indicate that p-H_2 and helicoptering o-H_2 prefer cationic sites, while cartwheeling o-H_2 prefers anionic sites.

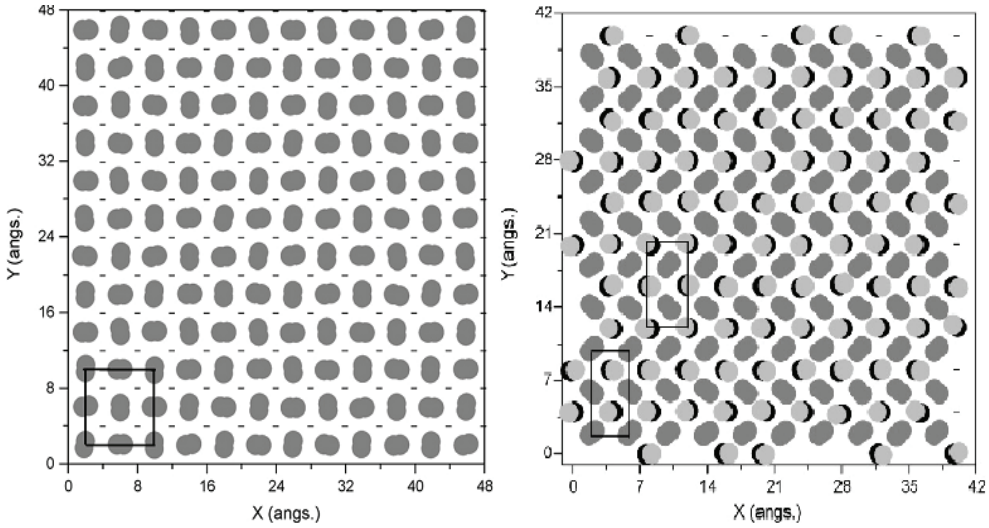

Fig. 11. The LiF(001) surface covered with H_2 molecules at 1 K. The (blue) symbol represents a Li^+ ion and the (yellow) symbol represents a F^-ion. The hydrogen atoms of molecules are shown in white color. $p(8\cdot2)$ structure shown in the right image, $p(4\cdot2)$ structure shown in the middle image and $p(2\cdot2)$ structure shown in the left image.

Monte Carlo simulations show that D_2 adopt a sequence of $c(n\times2)$ structures. The $c(2\times2)$ structure consists of an array of molecules covering every other Mg^{2+} site of the surface in a checkerboard pattern, with quantum mechanical delocalisation of the molecular axes eliminating azimuthal differences between molecules. Specifically, the o*rtho* and helicoptering *para* states are allowed to adsorb here. The $c(4\times2)$ structure consists of two kinds of adsorption sites. One third of the molecules adsorb directly over Mg^{2+} ions with a preference for a horizontal orientation for the molecular axes (o*rtho* or helicoptering *para*-states), while the remaining two thirds adsorb near, but are offset from, the O^{2-} ions with orientations that prefer a tilt from the surface normal. In terms of rotational states these are thought to be a mix of cartwheeling and helicoptering *para*-states or possibly skewed *ortho*-states. The tilted molecules sit 0.5 Å further from the surface than the horizontal molecules. The $c(6\times2)$ structure is an extension of the $c(4\times2)$ structure with only $1/5^{th}$ of the molecules adopting a horizontal orientation; the rest are tilted near O^{2-} ions.

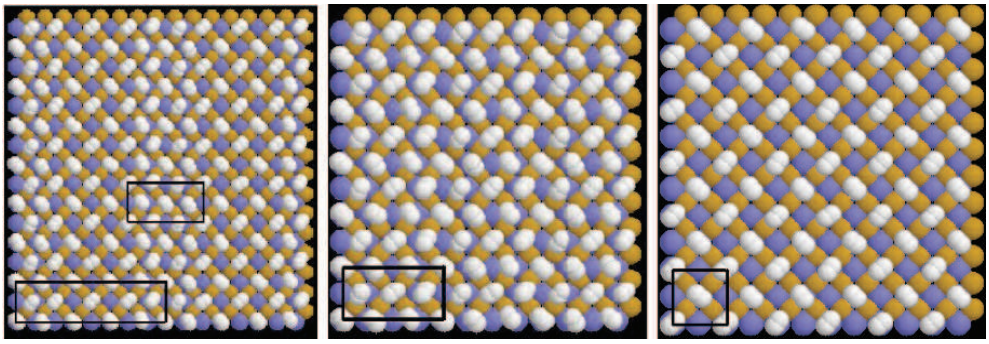

Fig. 10. The LiF(001) surface covered with H2 molecules at 1 K. The (blue) symbol represents a Li^+ ion and the (yellow) symbol represents a F^-ion. The hydrogen atoms of molecules are shown in white color. $p(8\times2)$ structure shown in the right image, $p(4\times2)$ structure shown in the middle image and $p(2\times2)$ structure shown in the left image.

6. Grand Canonical Monte Carlo (GCMC) simulation for CO_2 on MgO(001)

The adsorption isotherms of CO_2 on MgO ia obtained using Grand Canonical Monte Carlo (GCMC) simulations and ompared with experiment, as well as to explore the possible formation of monolayers of different densities [42]. The Canonical Monte Carlo (GCMC) refers to a simulation when the system at fixed temperature T, volume V and chemical potential δ. The chemical potential of the gas above the surface layer of the adsorbed molecules is in equilibrium with the adsorbed molecules:

$$\delta_{.surface}=\delta_{gas.} \tag{36}$$

If the gas is considered be ideal, the relation between the chemical potential and the pressure of the adsorbed molecules is

$$\delta_{molecules}=k_BT\ \ln(P\varpi^3/k_BT) \tag{37}$$

Where ϖ is the thermal de Broglie wavelength and kB is the Boltzmann constant. The GCMC simulations are actually performed at constant *B*, *V*, and *T*, where *B* is the so-called Adams parameter defined as

$$\delta = k_B T\, B - k_B T \ln(\varpi^3 / V) \tag{38}$$

The required relation for GCMC simulations is given as

$$B = \ln(P\varpi 3 / kBT) \tag{39}$$

The formation of a high density monolayer of CO2 on MgO(001) has been successfully simulated.

7. Conclusion

Histry and basics of Monte Carlo methods are discussing in the beging of this chapter. Then we give methods for describing the coordinate system and potentials that govern the interaction of adsorbed molecules with surfaces. The use of Monte Carlo methods to test the modern theory of phase transition in real systems have been explained. Statistical techniques to analyze the data obtained from simulations have been discusesed. Applications of Monte Carlo simulation of the real physical systems is discussed in details: e.g. N2, H2 and D2 adsorbed on NaCl(001), H2, D2 and N2 adsorbed on LiF(001), CO, CO2 H2 and D2 adsorbed on MgO(001).

8. References

[1] M.P. Allen and D. J. Tildesley, Computer Simulation of Liquids, Clarendon Press, Oxford, 1987.
[2] M.P. Allen and D. J. Tildesley, Computer Simulation in Chemical Physics, Kluwer Academic Publishers, Dordrecht (1993).
[3] M. E. J. Newman and G. T. Barkema, Monte Carlo Methods in Statistical Physics, Clarendon Press, Oxford (1999).
[4] Kalos and Whitlock. Monte Carlo Methods, Volume I: Basics. John Wiley & Sons, 1986.
[5] Hammersley and Handscomb. Monte Carlo Methods. John Wiley & Sons, 1965.
[6] Jerome Spanier and Ely M. Gelbard. Monte Carlo principles and neutron transport problems. Reading, Mass., Addison-Wesley Pub. Co, 1969.
[7] Christian P. Robert and George Casella. Monte Carlo Statistical Methods. Springer-Verlag, 2nd edition, 2004.
[8] A. Hall. On an experimental determination of Pi. Messeng. Math., 2:113–114, 1873.
[9] N. Metropolis and S. Ulam. The Monte Carlo method. Journal of the American Statistical Association, 44:335–341, 1949.
[10] D. Nicholson and N. G. Parsonage, Computer Simulation and Statistical Mechanics of adsorption, Academic Press, New York (1982).
[10] N. Metropolis, A. W. Rosenbluth, M. N. Rosenbluth, A. H. Teller, and E.Teller, J. Chem. Phys. 21,1078(1953).

[11] J. J. Binney, N. J. Dowrick, A. J. Fisher and M. E. J. Newman, The Theory of Critical Phenomena an Introduction to the Renormalization Group, Oxford University Press (1992).
[12] K. Binder, D. W. Hermann, Monte Carlo Simulations in Statistical Physics an Introduction, Springer-Verlag, Berlin (1992).
[13] Polanyi, Williams and O'Shea, J. Chem. Phys. 94,978 (1991)
[14] W. Hu, M.-A. Saberi, A. Jakalian, and D. B. Jack, J. Chem. Phys. 106, 2547 (1997).
[15] N.-T. Vu, A. Jakalian, and D. B. Jack, J. Chem. Phys. 106, 2551 (1997).
[16] N. –T. Vu and D. B. Jack, J. Chem. Phys. 108, 5653 (1998).
[17] A. K. Sallabi and D. B. Jack, J. Chem. Phys. 112, 5133 (2000).
[18] A. K. Sallabi and D. B. Jack. Phys. Rev. B 62, R4841 (2000).
[19] A. K. Sallabi ,J. N. Dawoud , and D. B. Jack, Applied Surface Science 256,2974(2010).
[20] J. N. Dawoud , A. K. Sallabi and D. B. Jack, Applied Surface Science 254, 7807(2008)
[21] J. N. Dawoud, A. K. Sallabi, I. I. Fasfous, D. B. Jack,ejournal of Surface Science and Nanotechnology 7,207 (2009).
[22] J. N. Dawoud , A. K. Sallabi and D. B. Jack, Surface Science 601, 3731(2007).
[23] Jamal Dawouda, Abdulwahab Sallabib, Ismail Fasfousa, and David Jack,Jordan Journal of Chemistry. 3,269(2008).
[24] W, Hu, M.Sc. Thesis, Concordia University (1997).
[25] A. B. MacIsaac, J. P. Whithead, K. De'Bell, and P. H. Poole, Phys. Rev. Lett. 77, 739 (1996).
[26] K. Binder, Annu. Rev. Phys. Chem. 37, 401 (1992).
[27] K. Binder, Phys. Rev. Lett. 47, 693 (1981).
[28] J. C. Polany and J. Williams, J. Chem. Phys. 94, 978 (1991).
[29] V. J. Barcaly, D. B. Jack, J. C. Polanyi, and Y. Zeiri, J. Chem. Phys. 97, 9458 (1992).
[30] M. A. Sabri, M. Sc. Thesis, Concordia University (1996).
[31] M. Karplus and R. N. Porter, Atoms and Molecules(Benjamin/Cummings, Menlo Park, 1970).
[32] F. Mulder, G. F. Thomas, and W. J. Meath, Mol. Phys. 41, 249 (1980).
[33] A. W. Meredith and A. J. Stone, J. Chem. Phys. 104, 3058 (1996).
[34] J. E. Lennard-Jones and B. M. Dent, Trans. Farad. Soc. 24, 92 (1928).
[35] W. A. Steele, The Interaction of Gases with Solid Surfaces (Pergamon press, Oxford,1974).
[36] T. Tang and J. P. Toennies, Z. Phys. D, 1, 91 (1986).
[37] Habitz, P., Tang, K. T., Toennies, J. P., Chem. Phys. Lett. 85, 461 (1982).
[38] C. Douketis, G. Scoles, S. Marchetti, M. Zen, and A. Thakkar, J. Chem. Phys. 76, 3057 (1982).
[39] T. L. Gilbert, J. Chem. Phys. 49, 2640 (1968).
[40] T. L. Gilbert, O. C. Simpson, and M. A. Williamson, ibid 63, 4061 (1975).
[41] F. T. Smith, Phys. Rev. A 5, 1708 (1972).
[42] Christopher D. Daub, G. N. Patey, D. B. Jack and A. K. Sallabi, "Monte Carlo simulations of the adsorption of CO2 on the MgO(100) surface" J. Chem. Phys.124, 114706 (2006).
[43] L. D. Roelofs and P. J. Estrup, Surf. Sci. 125, 51 (1983).

[44] J. M. Yeomans, Statistical Mechanics of Phase Transitions, Clarendon Press, Oxford (1992).
[45] J. V. José, L. P. Kadanoff, S. Kirkpatrick, and D. R. Nelson, Phys. Rev. B 16, 1217 (1977).
[46] G. Y. Hu and S. C. Ying, Physica 140A, 585 (1987).

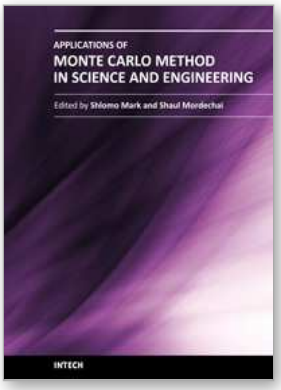

Applications of Monte Carlo Method in Science and Engineering
Edited by Prof. Shaul Mordechai

ISBN 978-953-307-691-1
Hard cover, 950 pages
Publisher InTech
Published online 28, February, 2011
Published in print edition February, 2011

In this book, Applications of Monte Carlo Method in Science and Engineering, we further expose the broad range of applications of Monte Carlo simulation in the fields of Quantum Physics, Statistical Physics, Reliability, Medical Physics, Polycrystalline Materials, Ising Model, Chemistry, Agriculture, Food Processing, X-ray Imaging, Electron Dynamics in Doped Semiconductors, Metallurgy, Remote Sensing and much more diverse topics. The book chapters included in this volume clearly reflect the current scientific importance of Monte Carlo techniques in various fields of research.

INTECH
open science | open minds

InTech Europe
University Campus STeP Ri
Slavka Krautzeka 83/A
51000 Rijeka, Croatia
Phone: +385 (51) 770 447
Fax: +385 (51) 686 166
www.intechopen.com

InTech China
Unit 405, Office Block, Hotel Equatorial Shanghai
No.65, Yan An Road (West), Shanghai, 200040, China
中国上海市延安西路65号上海国际贵都大饭店办公楼405单元
Phone: +86-21-62489820
Fax: +86-21-62489821